IEEE Access
Multidisciplinary ⋮ Rapid Review ⋮ Open Access Journal

Received March 23, 2020, accepted April 5, 2020, date of publication April 10, 2020, date of current version April 27, 2020.

Digital Object Identifier 10.1109/ACCESS.2020.2987051

A Day-Ahead Scheduling of Equivalent Energy Storage Model Considering Minimum-On-Off Time

MENG ZHANG[1], YU-QING BAO[1], (Member, IEEE), XUE-HUA WU[2], AND ZHEN-YA JI[1]
[1]NARI School of Electrical Engineering and Automation, Nanjing Normal University, Nanjing 210023, China
[2]School of Electrical Engineering, Southeast University, Nanjing 210096, China

Corresponding author: Yu-Qing Bao (baoyuqing@njnu.edu.cn)

This work was supported by the National Natural Science Foundation of China under Grant 51707099.

ABSTRACT In order to make Thermostatically Controlled Loads (TCLs) better meet the scheduling requirements, a day-ahead scheduling of equivalent energy storage model that takes into account of the minimum-on-off time is established. By considering the minimum-on-off time, the charging and discharging power, as well as the energy storage are modified, and the relationship between heat exchange power and energy storage are developed. By this way, the equivalent energy storage model more accurately reflects the real thermodynamic characteristic of TCLs and enables TCLs to exert the actual potential to participate in the scheduling. Finally, the simulation results verify the feasibility of the proposed scheduling method.

INDEX TERMS Thermostatically controlled loads, equivalent energy storage model, minimum-on-off time, day-ahead scheduling.

NOMENCLATURE

A. SETS AND INDICES

j	Index of generators
i	Index of thermostatically controlled loads (TCLs)
d	Index of load nodes
l	Index of branches
w	Index of wind farms

B. PARAMETERS

n	The total number of TCLs
R	Equivalent thermal resistance
C	Equivalent thermal capacity
Δt	Time step
$T_{\min}, T_{\max}$	The minimum and maximum value of the indoor temperature
T_{set}	The setting value of indoor temperature
T_{a}	Outdoor temperature
ε	Temperature control dead-band
$t_{\text{on}}, t_{\text{off}}$	The running and stopping time of compressors
$t_{\text{on,min}}, t_{\text{off,min}}$	The minimum of on/off time
T_{on}	Indoor temperature at time $t_{\text{on,min}}$
T_{off}	Indoor temperature at time $t_{\text{off,min}}$
F	The cost of power operation
N_{t}	The total period of time
N_{G}	The total number of generator units
N_{D}	The total number of load nodes
$QG_{l,j}$, $QW_{l,w}$, $QD_{l,d}$	Branches-generators, branches-wind farms, branches-load nodes incidence matrix
N_{w}	The total number of wind farms
η_i	The energy efficiency ratio of the i th TCL
a_1, a_2, a_3	The fuel cost coefficients of units
$c_{\text{SU}}, c_{\text{SD}}$	The unit prices of start-up and shut-down
c_{WC}	The unit price of wind curtailment
$P_{\text{G},j}^{\max}, P_{\text{G},j}^{\min}$	The upper and lower limit of the output power of the j th unit
c_{TCL}	The unit price of increasing or decreasing using TCLs
SU_j, -SD_j	The upper and lower limit of the ramp rate of the j th unit
$E_{\text{agg}}^{\max}, E_{\text{agg}}^{\min}$	The maximum and minimum value of energy storage
PLM_l	The maximum value of lth branch power flow

The associate editor coordinating the review of this manuscript and approving it for publication was Behnam Mohammadi-Ivatloo.

C. VARIABLES

$T_{\mathrm{in},t}$	Indoor temperature at time t
s_t	The on/off state of a TCL at time t
$P_{\mathrm{DR},d,t}$	The demand response power of the dth load node at time t
$P_{\mathrm{base},t}$	The baseline load power at time t
$P_{\mathrm{a,agg}}$	The aggregated average power
$P_{\mathrm{e},i,t}$	The actual electric power of the ith TCL at time t
$P_{\mathrm{e,agg},t}$	The actual aggregated electric power at time t
$P_{\mathrm{ex},i,t}$	The heat exchange power of the ith TCL at time t
$P_{\mathrm{ex,agg},t}$	The aggregated heat exchange power at time t
$P_{\mathrm{c,agg},t}$	The aggregated charging and discharging power at time t
$P_{\mathrm{c,down},t}$, $P_{\mathrm{c,up},t}$	The upper and lower limit of charging and discharging power at time t
$E_{i,t}$	The energy storage of the ith TCL at time t
$E_{\mathrm{agg},t}$	The aggregated energy storage at time t
$P_{G,j,t}$	The output power of the jth unit at time t
$D_{d,t}$	The power of the dth load node at time t
$PL_{l,t}$	Power flow of the lth branch at time t
$f_1(P_{\mathrm{G},j,t})$	The fuel cost of generator units
$f_2(SU_{j,t}), f_3(SD_{j,t})$	The costs of start-up and shut-down
$u_{j,t}$	The state of the jth unit at time t
$x_{j,t}$, $y_{j,t}$	The start-up and shut-down operation of the jth unit at time t
$P_{\mathrm{WC},w,t}$	The wind curtailment power of the wth wind farm at time t, where WC indicates wind curtailment
$f_4(P_{\mathrm{WC},w,t})$	The cost of wind curtailment
$f_5(P_{\mathrm{DR},d,t})$	The compensation cost of TCLs
$P_{\mathrm{W},w,t}$	The forecasted wind power of the wth wind farm at time t

I. INTRODUCTION

The development of economy and society leads to the prominent problems of resources and environment, and the utilization of new energy has become an important way to solve such problems. However, the continuous penetration of new energy has brought great challenges to the power system operation [1], [2]. Based on smart grid technologies, demand response (DR) can not only accommodate fluctuation of new energy sources, but also play an important role in improving the utilization of resources in the power grid [3]–[7].

As one of the important resources on the demand side, it is of great practical significance to study how to integrate large numbers of thermostatically controlled loads (TCLs) into the power system operation effectively.

Because of the complex thermodynamic characteristic of TCLs, they are difficult to participate in the scheduling problem, based on which some scheduling strategies are proposed in [8]–[10]. In [8], a TCLs scheduling scheme for residential users and commercial buildings is proposed. However, this scheme can only be applied to smart homes or smart buildings with small account of TCLs. An optimal conference scheduling method with minimum energy consumption is applied to commercial buildings with air conditioning system in [9]. In [10], a day-ahead scheduling model based on the self-adaptive TCL grouping method is proposed. However, this method does not consider the heterogeneity of massive TCLs.

The energy storage characteristics of TCLs have attracted attention, and the energy storage model is a better way to describe such energy storage characteristics. Several energy storage models for TCLs are proposed in [11]–[15]. In [11], for the inverter air conditioner, a thermal battery model is established to facilitate its participation in power system scheduling. In [12], an improved energy storage model is proposed when the parameters of TCLs are inconsistent and there is no short-cycling requirement. The energy storage models in [13], [14] use the average power to calculate the power, ignoring the time-varying power, the upper and lower limits of the power constraint are fixed value. In [15], the time-varying heat exchange power is adopted, but the minimum-on-off time is not considered, which leads to the low accuracy of the energy storage model.

Though some of the above literature establishes an equivalent energy storage model for the aggregated TCLs with heterogeneous parameters by introducing the heat exchange power instead of the average power, to reflect the time-varying characteristics. However, these models do not consider the minimum-on-off time, resulting in deviations in the day-ahead scheduling model.

To fill this gap, this paper introduces the minimum-on-off time into the energy storage model, redefines charging and discharging power constraints, energy storage constraints, and the relationship between heat exchange power and energy storage, so that the current energy storage model can make TCLs better participate in the power system scheduling, fully exert its potential and be more conducive to the stable and safe operation of the system.

The differences between the proposed method and existing works are listed in Table 1.

This paper is structured as follows: The day-ahead scheduling model and equivalent energy storage model are described in Section II. Section III introduces the innovation of this paper, that is, the energy storage model considering the minimum-on-off time. Section IV develops the case studies. Finally, Section V concludes the paper.

II. DAY-AHEAD SCHEDULING MODEL AND EQUIVALENT ENERGY STORAGE MODEL

Because of the increasing penetration of the renewable energy, its uncertainty and fluctuation impose great challenges to the power system operation. The participation of

TABLE 1. The differences between the proposed method and existing works.

Methods	Energy storage model	Time-varying heat exchange power	Minimum-on-off time
Reference [11]-[14]	Considered	Not Considered	Not Considered
Reference [15]	Considered	Considered	Not Considered
The proposed method	Considered	Considered	Considered

TCLs in the power system operation is beneficial to accommodate the fluctuation of new energy sources and improve the reliability of power system operation.

A. OPTIMIZATION MODEL CONSIDERING TCLs

Considering renewable energy sources such as wind power, the equivalent energy storage model of large-scale TCLs is introduced into the day-ahead scheduling model, taking the economic optimization as the objective function, which is defined as following:

$$\min F = \sum_{t=1}^{N_t}\sum_{j=1}^{N_G}\left(f_1(P_{G,j,t})+f_2(SU_{j,t})+f_3(SD_{j,t})\right) + \sum_{t=1}^{N_t}\sum_{w=1}^{N_W} f_4(P_{WC,w,t}) + \sum_{t=1}^{N_t}\sum_{d=1}^{N_D} f_5(P_{DR,d,t}) \tag{1}$$

$$f_1(P_{G,j,t}) = a_{1,j} + a_{2,j}\cdot P_{G,j,t} + a_{3,j}\cdot P_{G,j,t}^2 \tag{2}$$

$$f_2(SU_{j,t}) = c_{SU}\cdot x_{j,t} \tag{3}$$

$$f_3(SD_{j,t}) = c_{SD}\cdot y_{j,t} \tag{4}$$

$$f_4(P_{WC,w,t}) = c_{WC}\cdot P_{WC,w,t} \tag{5}$$

$$f_5(P_{DR,d,t}) = c_{TCL}\cdot P_{DR,d,t} \tag{6}$$

If $P_{DR,d,t}$ is positive, it means the load is shifted from time t to other time; if it is negative, it means the load is shifted from other time to time t.

The optimal scheduling problem is subjected to the following constraints.

(1) Power balance constraint

$$\sum_{j=1}^{N_G} P_{G,j,t} + \sum_{w=1}^{N_W}(P_{W,w,t} - P_{WC,w,t}) = \sum_{d=1}^{N_D} D_{d,t} - \sum_{d=1}^{N_D} P_{DR,d,t} \tag{7}$$

(2) On-off state of units

$$u_{j,t} = \begin{cases} 1 & \text{unit is on} \\ 0 & \text{unit is off} \end{cases} \tag{8}$$

(3) Start-up and shut-down variables of units

$$\begin{aligned} x_{j,t} - y_{j,t} &= u_{j,t} - u_{j,t-1} \\ x_{j,t} + y_{j,t} &\le 1 \end{aligned} \tag{9}$$

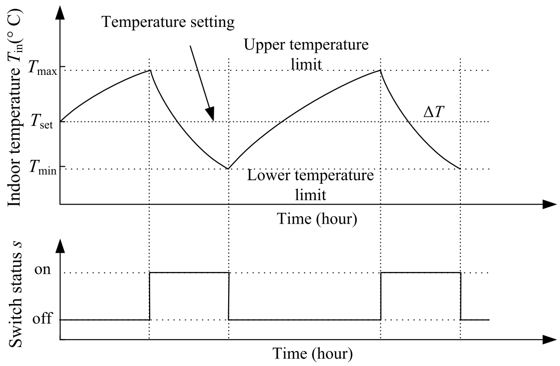

FIGURE 1. TCL duty cycle (refrigeration mode).

(4) Output power constraint of the units

$$u_{j,t}\cdot P_{G,j}^{\min} \le P_{G,j,t} \le u_{j,t}\cdot P_{G,j}^{\max} \tag{10}$$

(5) Ramp rate constraint of units

$$-SD_j \le P_{G,j,t} - P_{G,j,t-1} \le SU_j \tag{11}$$

(6) Power flow constraint of branches

$$\begin{aligned} PL_{l,t} = &\sum_{j=1}^{N_G} QG_{l,j}\cdot P_{G,j,t} \\ &+ \sum_{w=1}^{N_W} QW_{l,w}\cdot(P_{W,w,t} - P_{WC,w,t}) \\ &+ \sum_{d=1}^{N_D} QD_{l,d}\cdot(-D_{d,t} + P_{DR,d,t}) \\ &-PLM_l \le PL_{l,t} \le PLM_l \end{aligned} \tag{12}$$

Based on the above formulas, the day-ahead scheduling model of a large number of TCLs is established. In order to make scheduling more accurate and reliable, the equivalent energy storage model is introduced into the day-ahead scheduling model.

B. ETP MODEL OF TCLs

According to references [16]–[18], the first-order ETP model can be defined as following:

$$T_{in,t+1} = T_{in,t}\cdot e^{-\Delta t/RC} + (1 - e^{-\Delta t/RC})\cdot(T_{a,t} - s_t\cdot QR) \tag{13}$$

As shown in Fig. 1, when TCL is in the refrigeration mode, the indoor temperature rises to the upper temperature limit T_{max}, and TCL is switched on, which makes the indoor temperature drops. When the temperature drops to the lower temperature limit T_{min}, the TCL is switched off. By this way, the indoor temperature is kept within the temperature deadband $[T_{min}, T_{max}]$.

According to Fig. 1, the relationship between the switching states of TCL and the indoor temperature is as following:

$$s_{t+1} = \begin{cases} 0 & T_{in,t+1} < T_{min} \\ 1 & T_{in,t+1} > T_{max} \\ s_t & \text{otherwise} \end{cases} \tag{14}$$

where $s = 1$ represents the on state; $s = 0$ represents the off state. $T_{\max}$ and $T_{\min}$ are usually expressed by $T_{\max} = T_{\text{set}} + \varepsilon/2$ and $T_{\min} = T_{\text{set}} - \varepsilon/2$.

C. CONVENTIONAL EQUIVALENT ENERGY STORAGE MODEL

In references [13], [14], the charging and discharging power $P_{\text{c,agg},t}$ of TCLs is calculated directly by using $P_{\text{a,agg}}$.

$$P_{\text{c,agg},t} = P_{\text{e,agg},t} - P_{\text{a,agg}} \tag{15}$$

The working mode of TCLs is periodically on/off switching. When the operating duty cycle of TCLs is steady-state, the average power $P_{\text{a,agg}}$ is calculated by the duty cycle of operation, and can be expressed by:

$$P_{\text{a,agg}} = \frac{t_{\text{on}}}{t_{\text{on}} + t_{\text{off}}} \cdot P_{\text{e,agg},t} \tag{16}$$

In eq. (15), $P_{\text{e,agg},t}$ can be expressed by eq. (17).

$$P_{\text{e,agg},t} = \sum_{i=1}^{n} P_{\text{e},i,t} \cdot s_i = \sum_{i=1}^{n} \frac{Q_i}{\eta_i} \cdot s_i \approx n \cdot \frac{Q_{\text{ave}}}{\eta} \cdot s_i \tag{17}$$

where Q_{ave} means the average value of Q_i.

$$Q_{\text{ave}} = \frac{1}{n} \sum_{i=1}^{n} Q_i \tag{18}$$

However, eq.(15) ignores the time-varying power, and $P_{\text{a,agg}}$ is a fixed value. Since the temperature changes with time, the average power also changes with temperature.

D. IMPROVED EQUIVALENT ENERGY STORAGE MODEL

In order to improve the accuracy of the model, In references [15], the average power is replaced by the heat exchange power to calculate the charging and discharging power.

The aggregated charging and discharging power of TCLs $P_{\text{c,agg},t}$ is expressed by eq. (19).

$$P_{\text{c,agg},t} = P_{\text{e,agg},t} - P_{\text{ex,agg},t} \tag{19}$$

In eq. (19), $P_{\text{e,agg},t}$ can be calculated in eq. (17) and $P_{\text{ex,agg},t}$ can be calculated in eq. (23).

The relationship between $P_{\text{c,agg},t}$ and $P_{\text{DR},t}$ is expressed by eq.(20).

$$-P_{\text{DR},t} = P_{\text{c,agg},t} \tag{20}$$

If $T_{\max}$ is taken as the minimum point of energy storage, the energy storage $E_{i,t}$ of ith TCL can be written as following:

$$E_{i,t} = \frac{C_i T_{\max,i}}{\eta_i} - \frac{C_i T_{\text{in},i,t}}{\eta_i} = \frac{C_i (T_{\max,i} - T_{\text{in},i,t})}{\eta_i} \tag{21}$$

According to eq. (21), the relationship between $P_{\text{ex},i,t}$ and $E_{i,t}$ is expressed by eq. (22).

$$P_{\text{ex},i,t} = \frac{T_{\text{a},i,t} - T_{\text{in},i,t}}{\eta_i R_i} = \frac{T_{\text{a},i,t} - \left(T_{\max,i} - \frac{E_{i,t}\eta_i}{C_i}\right)}{\eta_i R_i} \tag{22}$$

Furthermore, the aggregated heat exchange power of the TCLs $P_{\text{ex,agg},t}$ is defined by:

$$P_{\text{ex,agg},t} = \sum_{i=1}^{n} P_{\text{ex},i,t} = \frac{E_{\text{agg},t}}{C_{\text{ave}} R_{\text{ave}}} + n \cdot \left(\frac{T_{\text{a}} - T_{\max,\text{ave}}}{\eta R_{\text{ave}}} \right) \tag{23}$$

where E_{ave}, C_{ave}, R_{ave} and $T_{\max,\text{ave}}$ are the average values, which can be defined as following:

$$C_{\text{ave}} = \frac{n}{\sum_{i=1}^{n} \frac{1}{C_i}} \tag{24}$$

$$R_{\text{ave}} = \frac{n}{\sum_{i=1}^{n} \frac{1}{R_i}} \tag{25}$$

$$T_{\max,\text{ave}} = \frac{1}{n} \sum_{i=1}^{n} T_{\max,i} \tag{26}$$

The values of η and T_a of each TCL are nearly the same, therefore, here we assume that all the η and T_a are the same.

The change of energy storage ΔE of large-scale TCLs during Δt can be expressed by eq. (27).

$$\Delta E = E_{\text{agg},t+1} - E_{\text{agg},t} = (P_{\text{e,agg},t} - P_{\text{ex,agg},t})\Delta t \tag{27}$$

According to eq. (17), eq. (23) and eq. (27), the recursive relationship between $E_{\text{agg},t+1}$ and $E_{\text{agg},t}$ is defined by:

$$E_{\text{agg},t+1} = E_{\text{agg},t} + \left(n \cdot \frac{Q_{\text{ave}}}{\eta} - \frac{E_{\text{agg},t}}{C_{\text{ave}} R_{\text{ave}}} - n \cdot \left(\frac{T_{\text{a}} - T_{\max,\text{ave}}}{\eta R_{\text{ave}}} \right) \right) \Delta t \tag{28}$$

To sum up, the power of TCLs can be equivalent to the charging and discharging power, and the storage of heat / cool can be equivalent to the energy storage, thus establishing the energy storage model of large-scale TCLs. However, this model does not consider the minimum-on-off time, resulting in deviations in the day-ahead scheduling model.

III. ENERGY STORAGE MODEL CONSIDERING MINIMUM-ON-OFF TIME

In order to make the scheduling model more accurate, the proposed method introduces the minimum-on-off time into the energy storage model, and modifies the charging and discharging power constraints, energy storage constraints, and the relationship between heat exchange power and energy storage.

A. CHARGING AND DISCHARGING POWER CONSIDERING MINIMUM-ON-OFF TIME

When considering the minimum-on-off time, the TCL's dynamic of the indoor temperature is shown in Fig. 2. When TCL is in the "on" state, the available temperature range is: $[T_{\min}, T_{\text{on}}]$. Similarly, when TCL is in the "off" state, the available temperature range is: $[T_{\text{off}}, T_{\max}]$.

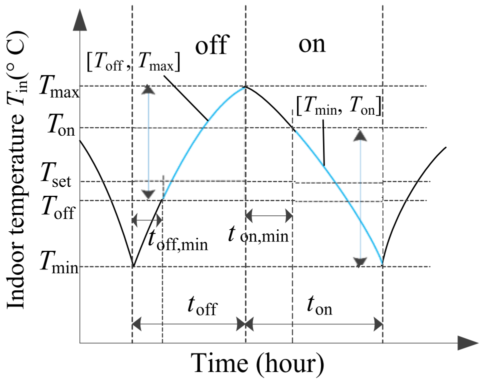

FIGURE 2. **Refrigeration mode with minimum-on-off time.**

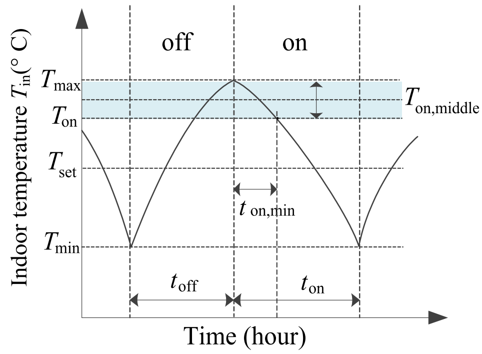

FIGURE 3. **Refrigeration mode with minimum-on time.**

When $P_{c,agg,t}$ is negative, the TCL needs to be turned off (TCL in "on" state). For the ith TCL in "on" state, the probability of being controlled is only:

$$\theta_1 = \frac{t_{ion} - t_{ion,min}}{t_{ion}} \tag{29}$$

Furthermore, combined with eq. (19), for a large number of TCLs, the actual available down load is:

$$P_{c,down,t} = (P^{min}_{e,agg,t} - P_{ex,agg,t}) \cdot \frac{t_{on,ave} - t_{on,\,min,ave}}{t_{on,ave}} \tag{30}$$

where $P_{ex,agg,t}$ is calculated according to eq. (23) and $t_{on,ave}$ can be calculated in eq. (31).

$$t_{on,ave} = -R_{ave}C_{ave}\ln(\frac{T_{min,ave} - T_a + Q_{ave}R_{ave}}{T_{max,ave} - T_a + Q_{ave}R_{ave}}) \tag{31}$$

According to eq. (17), the lower limit $P^{min}_{e,agg,t}$ in eq. (30) is obtained by setting all the TCLs off and it is usually set to 0:

$$P^{min}_{e,agg,t} = 0 \tag{32}$$

When $P_{c,agg,t}$ is positive, the TCL needs to be turned on (TCL in "off" state). For the ith TCL in "off" state, the probability of being controlled is only:

$$\theta_2 = \frac{t_{ioff} - t_{ioff,min}}{t_{ioff}} \tag{33}$$

Similarly, combined with eq. (19), for a large number of TCLs, the actual available up load is:

$$P_{c,up,t} = \left(P^{max}_{e,agg,t} - P_{ex,agg,t}\right) \cdot \frac{t_{off,ave} - t_{off,\,min,ave}}{t_{off,ave}} \tag{34}$$

where $P_{ex,agg,t}$ is calculated according to eq. (23) and $t_{on,ave}$ can be calculated in eq. (35).

$$t_{off,ave} = -R_{ave}C_{ave}\ln(\frac{T_{max,ave} - T_a}{T_{min,ave} - T_a}) \tag{35}$$

According to eq. (17), the upper limit $P^{max}_{e,agg,t}$ in eq. (34) can be obtained by setting all the TCLs on:

$$P^{max}_{e,agg,t} = n \cdot \frac{Q_{ave}}{\eta} \tag{36}$$

Finally, the constraint of $P_{c,agg,t}$ of TCLs participating in the scheduling can be defined by:

$$P_{c,down,t} \leq P_{c,agg,t} \leq P_{c,up,t} \tag{37}$$

where $P_{c,down,t}$ is derived from eq. (30), eq. (31) and eq. (32), as well as $P_{c,up,t}$ is derived from eq. (34), eq. (35) and eq. (36).

By this way, the minimum-on-off time can make $P_{c,agg,t}$ of TCLs closer to the actual value.

B. ENERGY STORAGE CONSIDERING MINIMUM-ON-OFF TIME

When considering the minimum-on-off time, the temperature change in the "on" range is shown in Fig. 3.

The minimum value of TCLs energy storage occurs when all TCLs are closed and the temperature is at the maximum value. When $t_{on,min}$ exists, only the TCLs whose temperature is within $[T_{min}, T_{on}]$ can be turned off. Therefore, when the temperature is distributed uniformly in the range $[T_{on}, T_{max}]$, the energy storage is the minimum value.

According to the eq. (13), $T_{on,ave}$ can be calculated in eq. (38).

$$T_{on,ave} = T_{max,ave} \cdot e^{-t_{on,min}/R_{ave}C_{ave}} + (1 - e^{-t_{on,min}/R_{ave}C_{ave}}) \cdot (T_a - Q_{ave}R_{ave}) \tag{38}$$

Further, $T_{on,middle,ave}$ can be written as following:

$$T_{on,middle,ave} = \frac{T_{on,ave} + T_{max,ave}}{2} \tag{39}$$

The minimum energy storage of individual TCL is:

$$E_{min,i} = \frac{C_i(T_{max,i} - T_{on,middle,i})}{\eta} \tag{40}$$

Then the minimum energy storage E^{min}_{agg} of large amounts of TCLs can be calculated by:

$$E^{min}_{agg} = \sum_{i=1}^{n} \frac{C_i(T_{max,i} - T_{on,middle,i})}{\eta} \approx n \cdot \frac{C_{ave}(T_{max,ave} - T_{on,middle,ave})}{\eta} \tag{41}$$

Similarly, the temperature change in the "off" range is shown in Fig. 4.

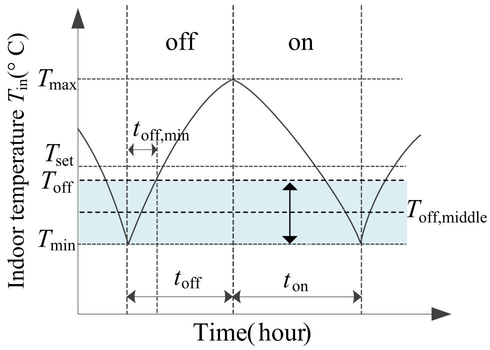

FIGURE 4. Refrigeration mode with minimum-off time.

The maximum value of TCLs energy storage occurs when all TCLs are opened and the temperature is at the minimum value. When $t_{off,min}$ exists, only the TCLs whose temperature is within $[T_{off}, T_{max}]$ can be turned on. Therefore, when the average temperature is at the midpoint of range $[T_{min}, T_{off}]$, the energy storage is the maximum value.

$T_{off,ave}$ can be calculated in eq. (42).

$$T_{off,ave} = T_{min,ave} \cdot e^{-t_{off,min}/R_{ave}C_{ave}} + (1 - e^{-t_{off,min}/R_{ave}C_{ave}}) \cdot T_a \quad (42)$$

$T_{off,middle,ave}$ can be calculated as following:

$$T_{off,middle,ave} = \frac{T_{off,ave} + T_{min,ave}}{2} \quad (43)$$

The maximum energy storage of individual TCL is:

$$E_{max,i} = \frac{C_i(T_{max,i} - T_{off,middle,i})}{\eta} \quad (44)$$

Then the maximum energy storage E_{agg}^{max} of large amounts of TCLs can be written as following:

$$E_{agg}^{max} = \sum_{i=1}^{n} \frac{C_i(T_{max,i} - T_{off,middle,i})}{\eta} \approx n \cdot \frac{C_{ave}(T_{max,ave} - T_{off,middle,ave})}{\eta} \quad (45)$$

Finally, The limits of the energy storage of aggregated TCLs participating in the scheduling are expressed by eq. (46).

$$E_{agg}^{min} \le E_{agg,t} \le E_{agg}^{max} \quad (46)$$

where E_{agg}^{min} is derived from eq. (38), eq. (39) and eq. (41), as well as E_{agg}^{max} is derived from eq. (42), eq. (43) and eq. (45).

The minimum-on-off time defines the upper and lower limits of $E_{agg,t}$ and makes it fluctuate within the actual range, which is conducive to exert the actual potential of TCLs to participate in the scheduling.

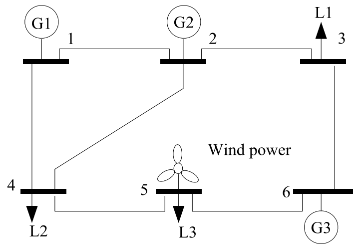

FIGURE 5. The six-bus system.

C. THE RELATIONSHIP BETWEEN $P_{ex,agg,t}$ AND $E_{agg,t}$

As it can be seen from eq. (22), $P_{ex,agg,t}$ of TCLs has a relationship with $E_{agg,t}$ and then the constraint between them can be obtained as eq. (47).

$$P_{ex,agg,t} = \sum_{i=1}^{n} P_{ex,i,t} = \frac{E_{agg,t}}{C_{ave}R_{ave}} + n \cdot \left(\frac{T_a - T_{max,ave}}{\eta R_{ave}}\right) \quad (47)$$

D. THE RELATIONSHIP BETWEEN $E_{agg,t+1}$ AND $E_{agg,t}$

According to eq. (27), the recursive relationship between $E_{agg,t+1}$ and $E_{agg,t}$ is defined by:

$$E_{agg,t+1} = E_{agg,t} + P_{c,agg,t} \cdot \Delta t \quad (48)$$

In the day-ahead scheduling model based on the proposed equivalent energy storage model, the constraints include not only the conventional constraints in the scheduling model, but also the relevant constraints of the TCLs energy storage model.

The constraints used in the optimization problem are as follows:

- Conventional constraints in the scheduling model, including eq. (1) ~ (12).
- Constraints of the proposed TCLs energy storage model (The relationship between $P_{c,agg,t}$, $E_{agg,t}$ and $P_{ex,agg,t}$):

1) The constraints of $P_{c,agg,t}$: including eq. (31) ~ (32) and eq. (35) ~ (37).
2) The constraints of $E_{agg,t}$:including eq. (38) ~ (39), eq. (41) ~ (43) and eq. (45) ~ (46).
3) The relationship between the $P_{ex,agg,t}$ and the limits of $P_{c,agg,t}$: including eq. (30) and eq. (34).
4) The relationship between $P_{ex,agg,t}$ and $E_{agg,t}$: including eq. (47).
5) The relationship between $E_{agg,t+1}$ and $E_{agg,t}$: including eq. (48).

IV. CASE STUDIES

In this paper, the nonlinear problems are transformed into linear problems by quadratic programming, MATLAB software and Matpower, Cplex, Yalmip tool packages are used for simulation.

A six-bus system is used for verification, as shown in Fig. 5. The system consists of three generator units G1, G2 and G3, respectively on bus 1, 2 and 6, and a wind farm on bus 5. The parameter of generator units refers to [19], [20]

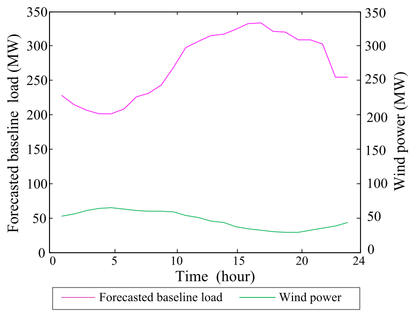

FIGURE 6. The forecasted load and wind power for six-bus system.

TABLE 2. Data of generator units in the six-bus system.

Units	Maximum output (MW)	Minimum output (MW)	Ramp rate (MW/h)	Energy consumption coefficient		
				a	*b*	*c*
G1	220	100	55	100	10.00	0.050
G2	100	10	50	162	40.66	0.001
G3	20	10	20	171	22.06	0.006

TABLE 3. The parameters of the TCLs.

Parameters	Mean value*	Relative standard deviation (RSD) of normal distributions
T_{set}	20° C	0.1
ε	0.625° C	0.1
T_a	32° C	0
R	2° C/kW	0.1
C	10 kWh/° C	0.1
Q	14kW	0.1
η	2.5	0

*Mean values refer to [21]

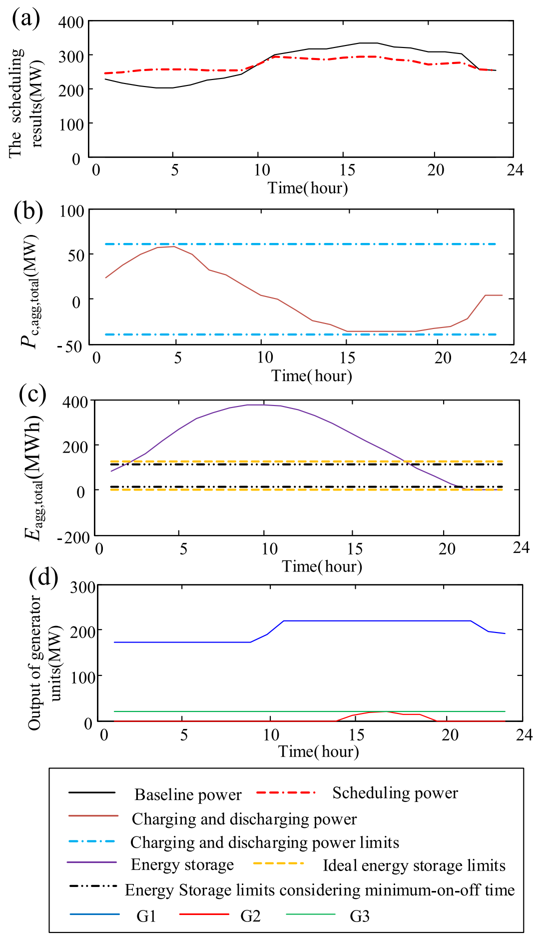

FIGURE 7. The scheduling results of Model 1. (a) Scheduling results. (b) $P_{c,agg,total}$. (c) $E_{agg,total}$. (d) Output of generator units.

and are listed in Table 2, the forecasted baseline load and wind power are shown in Fig. 6.

The case studies consist of 50000 TCLs. It is assumed that all TCLs are working in refrigeration mode. Considering the randomness of massive TCLs and heterogeneous parameter distribution, the parameters are set to random normal distribution, with the mean value and relative standard deviation are listed in Table 3, and the initial state of TCLs is assumed to be stable.

A. SCHEDULING RESULTS

For comparison, four scheduling models are developed as follows:

- Model 1: Traditional scheduling model: only $P_{c,agg,t}$ constraint of TCLs is considered and it is calculated by eq. (15), in which $P_{a,agg}$ is 120MW, calculated by eq. (16).
- Model 2: The scheduling model considers the TCLs equivalent energy storage model, but $P_{c,agg,t}$ is calculated by $P_{a,agg}$, the same as Model 1 (This method follows the idea of many existing methods [13], [14]).
- Model 3: The scheduling model considers TCLs equivalent energy storage model, and $P_{c,agg,t}$ is calculated through $P_{ex,agg,t}$. $P_{ex,agg,t}$ is calculated by eq. (23), then $P_{c,agg,t}$ is calculated by eq. (19) [15].
- Model 4: The scheduling considers minimum-on-off time, the charging and discharging power constraints in eq. (37), the energy storage constraints in eq. (46) and the relationship between heat exchange power and energy storage in eq. (47) are redefined.

The scheduling results are shown in Fig. 7~ Fig. 10.

From the four scheduling results, we can draw the following conclusions:

1) It can be seen from Fig. 7 that if the equivalent energy storage model is not considered, although the limit of $P_{c,agg,total}$(sum of charging and discharging power of all load nodes) is constrained, the maximum energy storage value reaches 400MWh, far exceeding the actual energy storage limit. This shows that in Model 1, TCLs are insufficient to meet the scheduling requirements.
2) Due to the different calculation methods of $P_{c,agg,t}$ in Model 3 and Model 4, the upper and lower limits of $P_{c,agg,total}$ in Fig. 7 (b) and Fig. 8 (b) are fixed values, while the upper and lower limits of $P_{c,agg,total}$ in Fig. 9 (b) and Fig. 10 (b) are time-varying.

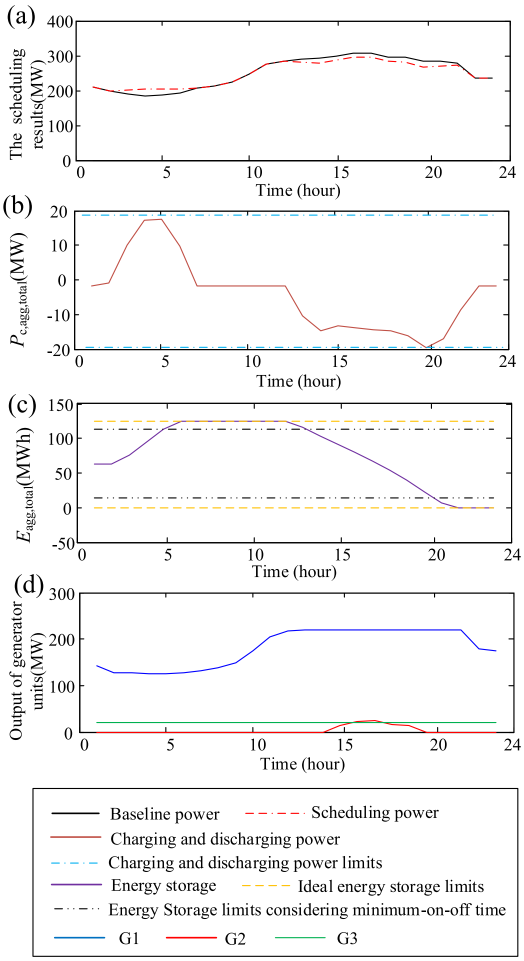

FIGURE 8. **The scheduling results of Model 2. (a) Scheduling results. (b) $P_{c,agg,total}$. (c) $E_{agg,total}$. (d) Output of generator units.**

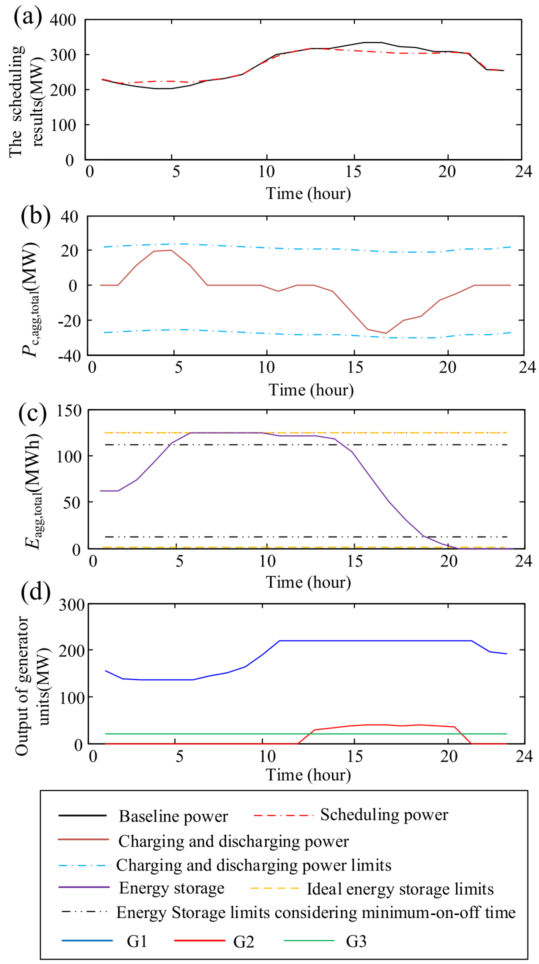

FIGURE 9. **The scheduling results of Model 3. (a) Scheduling results. (b) $P_{c,agg,total}$. (c) $E_{agg,total}$. (d) Output of generator units.**

3) Compared with Model 3 and Model 4, $E_{\text{agg,total}}$ (sum of energy storage of all load nodes) in Model 4 fluctuates within the range of actual energy storage, and $P_{\text{c,agg,total}}$ is closer to the actual value under the premise of considering the minimum-on-off time.
4) From Fig. 7∼ Fig. 10, it can be seen that the equivalent energy storage model considering the minimum-on-off time can limit the charging and discharging power, energy storage of TCLs to a safe range, exert the actual potential of TCLs to participate in the scheduling.

B. THE LOAD TRACKING CONTROL RESULTS

In order to verify effectiveness of the proposed scheduling model, load tracking control is adopted, so that the actual aggregated power of TCLs is as close as possible to the power of day-ahead scheduling. PI controller is used in the load tracking control. The four control models consider the minimum-on-off time.

The state of energy storage (*SOC*) at time t is defined as eq. (49).

$$SOC_t = \frac{E'_{\text{agg},t}}{E^{\max}_{\text{agg}}} \tag{49}$$

where $E\prime_{\text{agg},t}$ is the aggregated energy storage obtained by the tracking control.

In the following examples, the results of the load tracking control are compared, as shown in Fig. 11∼ Fig. 14.

From Fig. 11∼ Fig. 14, the following conclusions can be obtained.

1) In Fig. 11, because the equivalent energy storage model of TCLs is not considered in the scheduling Model 1, the load tracking control effect is very poor, and it can hardly be tracked. During 3 ∼ 18h and 21 ∼ 24h, *SOC* is either close to 1 or close to 0, which obviously shows that the potential of TCLs has been exhausted at this time and it is impossible to fully participate in power system scheduling.
2) In Fig. 12, the equivalent energy storage model is considered in the scheduling Model 2, but $P_{\text{c,agg},t}$ is calculated by $P_{\text{a,agg}}$. It can be seen from the figure that although the scheduling results in Fig. 12 can be tracked in most of the time, the tracking fails in 20 ∼ 24h, and its *SOC* is close to 0.
3) In Fig. 13, $P_{\text{c,agg},t}$ is calculated by $P_{\text{ex,agg},t}$, the tracking performance is a little better than Model 2, but it is not

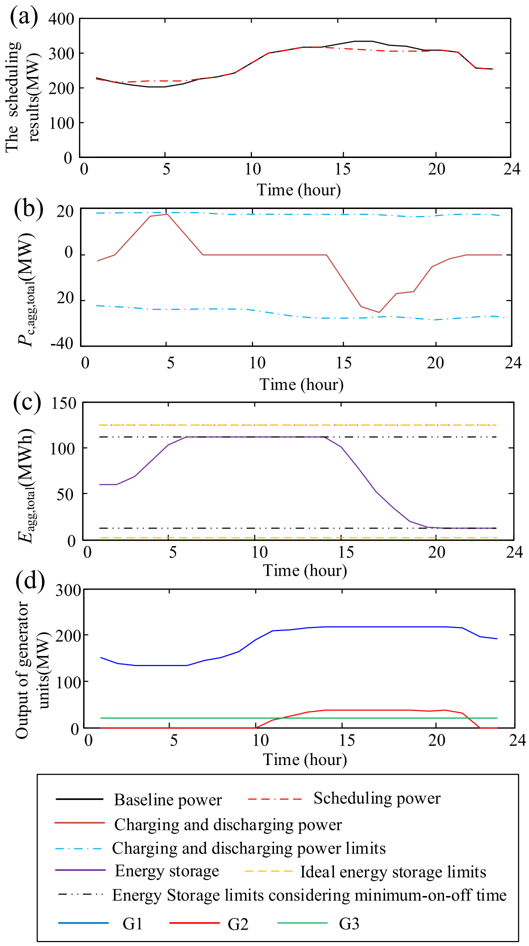

FIGURE 10. **The scheduling results of Model 4. (a) Scheduling results. (b) $P_{c,agg,total}$. (c) $E_{agg,total}$. (d) Output of generator units.**

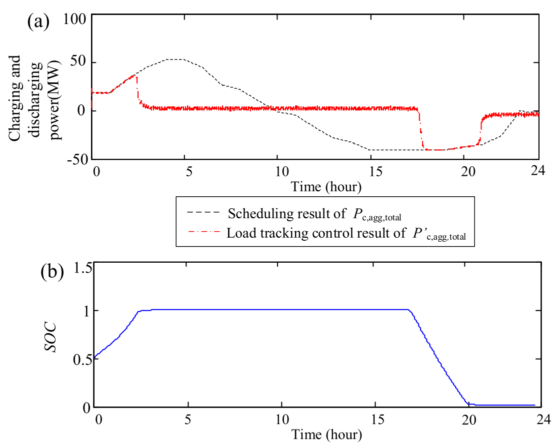

FIGURE 11. **The load tracking control results of Model 1. (a) Charging and discharging power. (b)SOC of the equivalent energy storage model.**

fully tracked. In 19 ∼ 24h, the load tracking fails, and the *SOC* is close to 0.

4) Fig. 14 shows the results of load tracking control using the proposed scheduling model. It can be seen from the figure that not only the power scheduling results

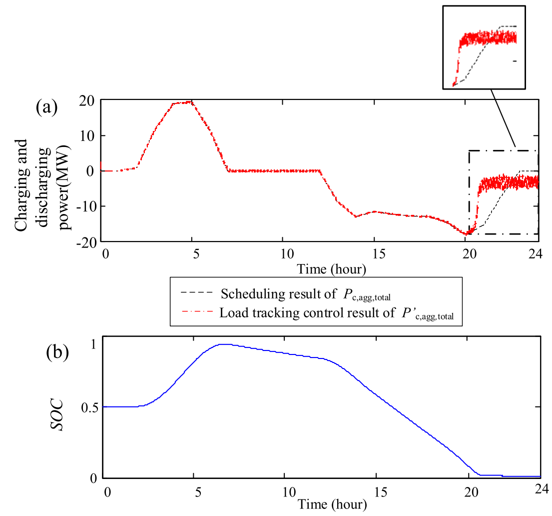

FIGURE 12. **The load tracking control results of Model 2. (a) Charging and discharging power. (b)SOC of the equivalent energy storage model.**

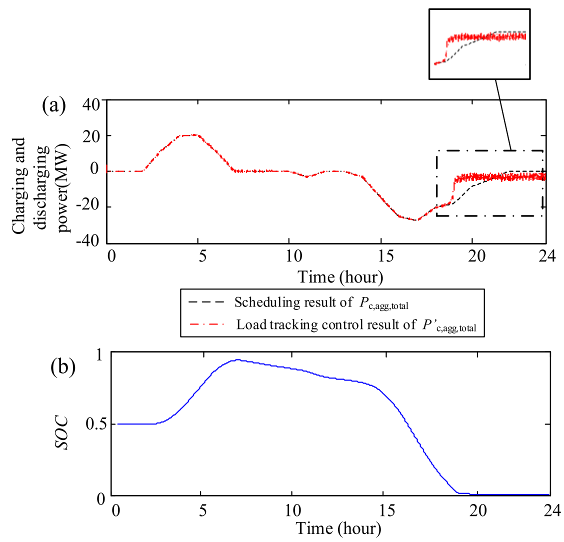

FIGURE 13. **The load tracking control results of Model 3. (a) Charging and discharging power. (b)SOC of the equivalent energy storage model.**

of large-scale TCLs can be tracked well, but also the *SOC* is always controlled within the range of 0 ∼1. This shows that considering the minimum-on-off time in the scheduling model to calculate the limits of charging and discharging power and energy storage are conducive to the stability of power system operation.

In order to clearly show the accuracy of the load tracking control results, the integrated square error (*ISE*) is adopted, as shown in eq. (50).

$$ISE = \int_0^T (P'_{c,agg,t} - P_{c,agg,t})^2 dt \tag{50}$$

where $P'_{c,agg,t}$ is the power obtained by the tracking control.

The results are shown in Table 4, from which it can be seen that *ISE* of Model 4 (the proposed model) is the smallest and

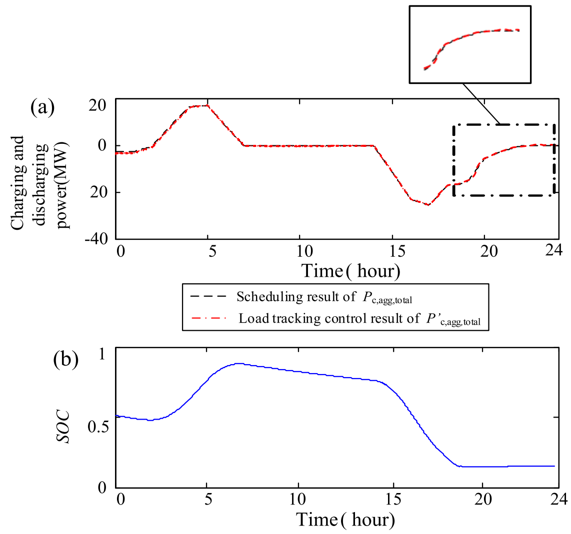

FIGURE 14. The load tracking control results of Model 4. (a) Charging and discharging power. (b)SOC of the equivalent energy storage model.

TABLE 4. ISE results of different load tracking control methods.

	Model 1	Model 2	Model 3	Model 4
ISE(MW)^2·h	2.2438×10^4	1.1785×10^2	75.2408	10.3277

far smaller than the other three models. This indicates that it is necessary to consider the minimum-on-off time, which can improve the accuracy of the model, so that TCLs can better meet the scheduling requirements.

C. VERIFICATION OF THE FEASIBILITY

In order to further verify the necessity of the minimum-on-off time in the scheduling model, the following two cases are compared.

- Case 1: Neither the scheduling model nor the control model considers the minimum-on-off time.
- Case 2: Both the scheduling model and the control model consider the minimum-on-off time.

The difference between this example and the previous one (Section IV, Subsection B) is that the previous control models all consider the minimum-on-off time, and this example is verified separately.

The temperature and switch status of Case 1 and Case 2 are compared, as shown in Fig. 15 and Fig. 16.

It can be seen from Fig. 15 that if the minimum-on-off time is not taken into account, the switching frequency is very high, up to once every one second, seriously affecting the lifetime of TCLs, which is inconsistent with the actual situation. However, if the minimum-on-off time is considered, as shown in Fig. 16, the switching frequency is obviously reduced and the lifetime of TCLs are therefore prolonged. This verifies the feasibility of the method proposed in this paper.

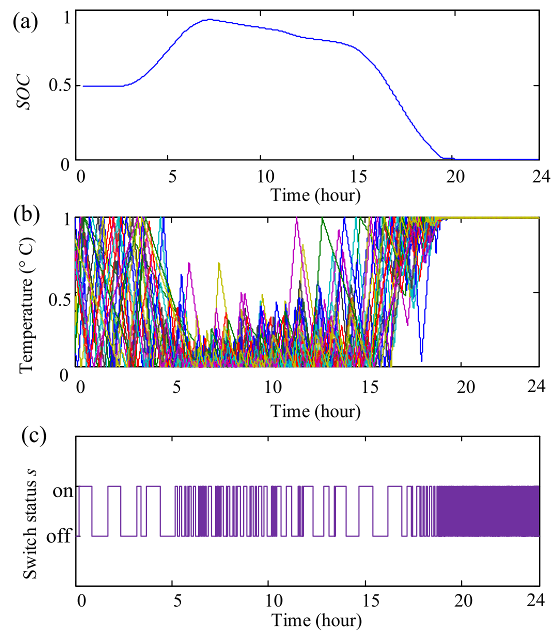

FIGURE 15. Simulation results of Model 3. (a)SOC of the equivalent energy storage model. (b)Temperature of randomly selected 20 TCLs. (c) Switch status of randomly selected one TCL.

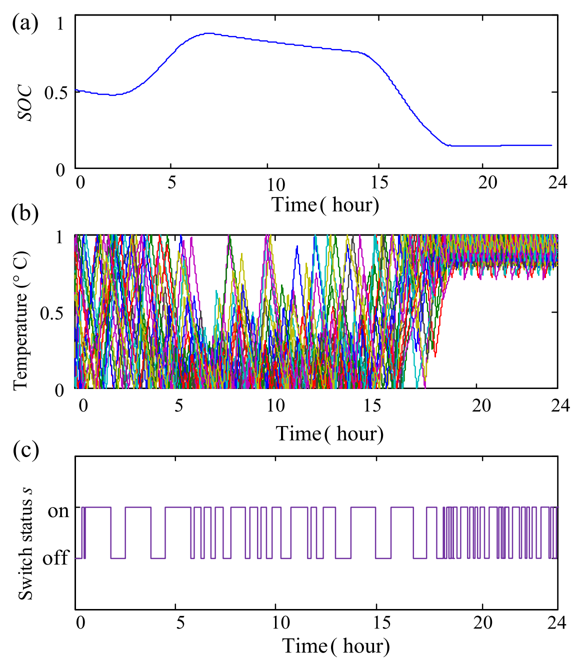

FIGURE 16. Simulation results of Model 4. (a)SOC of the equivalent energy storage model. (b)Temperature of randomly selected 20 TCLs (c) Switch status of randomly selected one TCL.

D. VERIFICATION OF 118-BUS SYSTEM

In this section, 118-bus system is used to verify Model 4 (the proposed mode). One million TCLs in the cooling mode are distributed at each load bus in proportion to the bus load. The scheduling results are shown in Fig. 17 and the load tracking control results are shown in Fig. 18.

From Fig. 17~Fig. 18, it can be seen that the proposed method successfully schedules the TCLs in the 118-bus

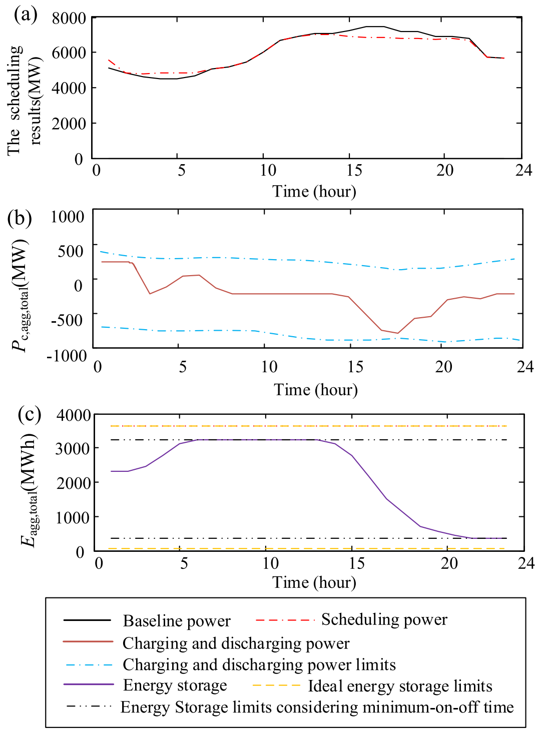

FIGURE 17. **The scheduling results of Model 4 based on 118-bus system. (a) Scheduling results. (b) Pc,agg,total. (c) Eagg,total.**

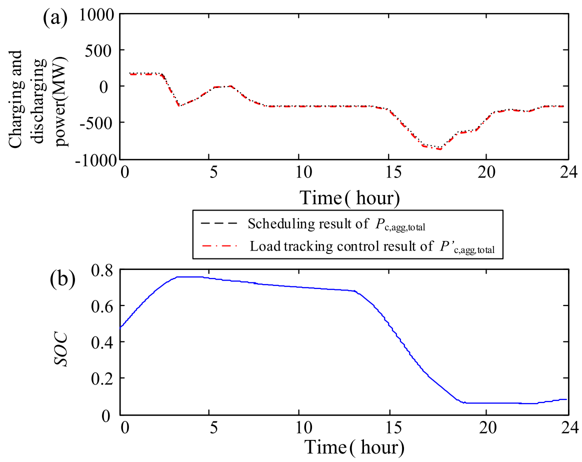

FIGURE 18. **The load tracking control results of Model 4 based on 118-bus system. (a) Charging and discharging power. (b)SOC of the equivalent energy storage model.**

system, and the load tracking control results verify the feasibility of the scheduling results.

V. CONCLUSION

In this paper, the minimum-on-off time is taken into account in equivalent energy storage model and the day-ahead scheduling model of TCLs, in order to make the scheduling more accurate. The main contributions are as follows:

1) An equivalent energy storage model of TCLs considering the minimum-on-off time is established. Compared with [15], the designed model can more accurately depict the actual dynamic of the TCLs.
2) The minimum-on-off time is taken into account in the day-ahead scheduling model of TCLs, based on which the constraints of charging and discharging power, energy storage are redefined, so that more accurate scheduling results can be obtained.

Through load tracking control, the scheduling results can be accurately tracked. It is shown that the scheduling model is more accurate when the minimum-on-off time is considered.

Future work will focus on the second-order ETP model and introduce it to the day-ahead scheduling model, in order to further improve the accuracy of scheduling.

REFERENCES

[1] C. Lowery and M. O'Malley, "Impact of wind forecast error statistics upon unit commitment," *IEEE Trans. Sustain. Energy*, vol. 3, no. 4, pp. 760–768, Oct. 2012.
[2] Y. Zhang, J. Wang, T. Ding, and X. Wang, "Conditional value at risk-based stochastic unit commitment considering the uncertainty of wind power generation," *IET Gener., Transmiss. Distrib.*, vol. 12, no. 2, pp. 482–489, Jan. 2018.
[3] J. Wu, B. Zhang, and Y. Jiang, "Optimal day-ahead demand response contract for congestion management in the deregulated power market considering wind power," *IET Gener., Transmiss. Distrib.*, vol. 12, no. 4, pp. 917–926, Feb. 2018.
[4] N. Lu and Y. Zhang, "Design considerations of a centralized load controller using thermostatically controlled appliances for continuous regulation reserves," *IEEE Trans. Smart Grid*, vol. 4, no. 2, pp. 914–921, Jun. 2013.
[5] S. Shao, M. Pipattanasomporn, and S. Rahman, "Demand response as a load shaping tool in an intelligent grid with electric vehicles," *IEEE Trans. Smart Grid*, vol. 2, no. 4, pp. 624–631, Dec. 2011.
[6] S. Ashok and R. Banerjee, "Optimal operation of industrial cogeneration for load management," *IEEE Trans. Power Syst.*, vol. 18, no. 2, pp. 931–937, May 2003.
[7] Z. Xu, J. Ostergaard, and M. Togeby, "Demand as frequency controlled reserve," *IEEE Trans. Power Syst.*, vol. 26, no. 3, pp. 1062–1071, Aug. 2011.
[8] Y.-Y. Hong, J.-K. Lin, C.-P. Wu, and C.-C. Chuang, "Multi-objective air-conditioning control considering fuzzy parameters using immune clonal selection programming," *IEEE Trans. Smart Grid*, vol. 3, no. 4, pp. 1603–1610, Dec. 2012.
[9] B. Chai, A. Costa, S. D. Ahipasaoglu, C. Yuen, and Z. Yang, "Optimal meeting scheduling in smart commercial building for energy cost reduction," *IEEE Trans. Smart Grid*, vol. 9, no. 4, pp. 3060–3069, Jul. 2018.
[10] F. Luo, Z. Y. Dong, K. Meng, J. Wen, H. Wang, and J. Zhao, "An operational planning framework for large-scale thermostatically controlled load dispatch," *IEEE Trans. Ind. Informat.*, vol. 13, no. 1, pp. 217–227, Feb. 2017.
[11] M. Song, C. Gao, H. Yan, and J. Yang, "Thermal battery modeling of inverter air conditioning for demand response," *IEEE Trans. Smart Grid*, vol. 9, no. 6, pp. 5522–5534, Nov. 2018.
[12] B. M. Sanandaji, H. Hao, K. Poolla, and T. L. Vincent, "Improved battery models of an aggregation of thermostatically controlled loads for frequency regulation," in *Proc. Amer. Control Conf.*, Portland, OR, USA, Jun. 2014, pp. 38–45.
[13] J. L. Mathieu, M. Kamgarpour, J. Lygeros, G. Andersson, and D. S. Callaway, "Arbitraging intraday wholesale energy market prices with aggregations of thermostatic loads," *IEEE Trans. Power Syst.*, vol. 30, no. 2, pp. 763–772, Mar. 2015.
[14] V. Trovato, S. H. Tindemans, and G. Strbac, "Security constrained economic dispatch with flexible thermostatically controlled loads," in *Proc. IEEE PES Innov. Smart Grid Technol., Eur.*, Oct. 2014, pp. 1–6.
[15] P. Chen, Y.-Q. Bao, X. Zhu, J. Zhang, and M. Hu, "Day-ahead scheduling of large numbers of thermostatically controlled loads based on equivalent energy storage model," *J. Modern Power Syst. Clean Energy*, vol. 7, no. 3, pp. 579–588, May 2019.
[16] C. H. Wai, M. Beaudin, H. Zareipour, A. Schellenberg, and N. Lu, "Cooling devices in demand response: A comparison of control methods," *IEEE Trans. Smart Grid*, vol. 6, no. 1, pp. 249–260, Jan. 2015.

[17] N. Lu, "An evaluation of the HVAC load potential for providing load balancing service," *IEEE Trans. Smart Grid*, vol. 3, no. 3, pp. 1263–1270, Sep. 2012.

[18] C. Perfumo, E. Kofman, J. H. Braslavsky, and J. K. Ward, "Load management: Model-based control of aggregate power for populations of thermostatically controlled loads," *Energy Convers. Manage.*, vol. 55, pp. 36–48, Mar. 2012.

[19] H. Wu, X. Guan, Q. Zhai, F. Gao, and Y. Yang, "Security-constrained generation scheduling with feasible energy delivery," in *Proc. IEEE Power Energy Soc. Gen. Meeting*, Jul. 2009, pp. 1–6.

[20] H. Wu, M. Shahidehpour, and M. E. Khodayar, "Hourly demand response in day-ahead scheduling considering generating unit ramping cost," *IEEE Trans. Power Syst.*, vol. 28, no. 3, pp. 2446–2454, Aug. 2013.

[21] D. S. Callaway, "Tapping the energy storage potential in electric loads to deliver load following and regulation, with application to wind energy," *Energy Convers. Manage.*, vol. 50, no. 5, pp. 1389–1400, May 2009.

MENG ZHANG was born in Anhui, China, in 1996. She received the B.S. degree from Anhui Jianzhu University, Hefei, China, in June 2019. She is currently pursuing the M.S. degree with Nanjing Normal University (NJNU). Her current research interest includes power system operation and scheduling.

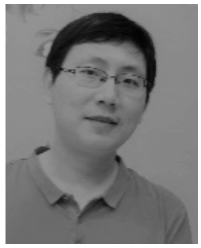

YU-QING BAO (Member, IEEE) was born in Zhenjiang, China, in 1987. He received the Ph.D. degree from Southeast University (SEU), Nanjing, China, in March 2016. He is currently an Associate Professor with Nanjing Normal University (NJNU). His current research interests include power system operation and scheduling, power demand side management, and the frequency control of the power systems.

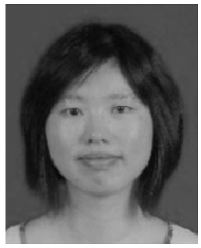

XUE-HUA WU received the B.S. degree in electrical engineering and the M.S. degree in power system and its automation from the Nanjing University of Aeronautics and Astronautics (NUAA), Nanjing, China, in 2009 and 2012, respectively. She is currently pursuing the Ph.D. degree in electrical engineering with Southeast University (SEU), Nanjing. Her research interest includes machine learning and its application in electrical engineering.

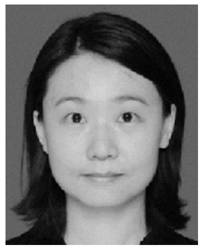

ZHEN-YA JI received the B.Eng. degree and Ph.D. degree in electrical engineering from Southeast University, Nanjing, China, in 2009 and 2018, respectively. She was a Visiting Student with Rheinisch-Westfälische Technische Hochschule Aachen, Germany, from 2012 to 2013. She has been an Assistant Professor with Nanjing Normal University, since 2018. Her research interests include demand side management and integrated energy systems.